

A layer-structured Eu-MOF as highly selective fluorescent probe for Fe^{3+} detection through cation-exchange approach

1. Crystal data for La(Y)L

Table S1. Cell parameters of all LnL .

$\text{C}_{35}\text{H}_{32}\text{NO}_{13}\text{Ln}$ ($\text{Ln} = \text{La}, \text{Y}, \text{Eu}, \text{Tb}, \text{Gd}$), Space group, P-1

Ln	$a / \text{\AA}$	$b / \text{\AA}$	$c / \text{\AA}$	$\alpha / {}^\circ$	$\beta / {}^\circ$	$\gamma / {}^\circ$	$V / \text{\AA}^3$
La	9.189(3)	11.486(4)	17.918(6)	80.253(6)	81.343(5)	86.819(5)	1841.8(11)
Y	9.3193(11)	11.8459(14)	17.601(2)	82.597(2)	82.102(2)	87.194(2)	1907.6(4)
Eu	9.25	11.64	18.01	80.39	81.40	87.11	1904.252
Tb	9.31	11.67	18.20	81.91	82.88	88.101	1910.328
Gd	9.26	11.54	18.21	80.981	81.55	88.21	1887.182

2. Luminescent Measurements

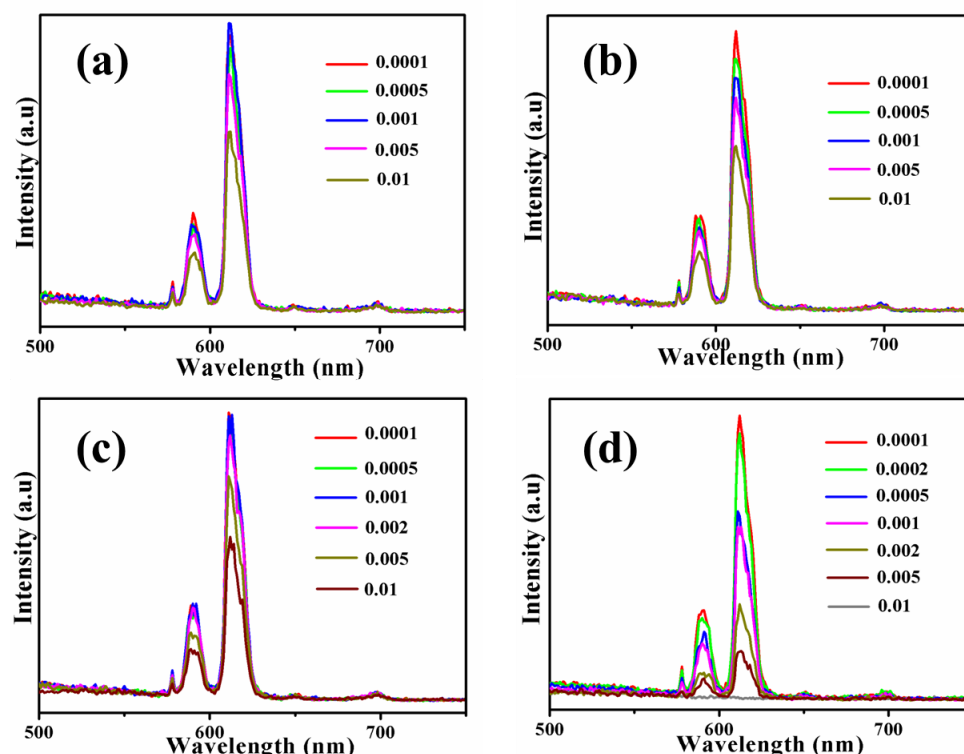


Fig. S1 Comparison of the emission intensity of $\text{M}^{n+}\text{-EuL}$ (a) Ag^+ , (b) Cu^{2+} , (c) Fe^{2+} , (d) Fe^{3+} immersing in different concentrations of $\text{M}(\text{NO}_3)_x$ aqueous solution, $\lambda_{\text{ex}} = 320$

nm.

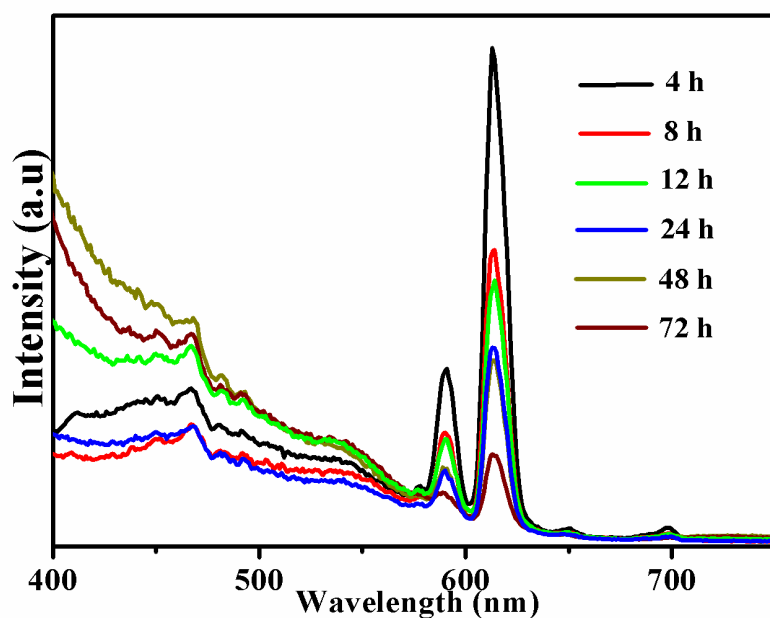


Fig. S2 PL emission spectra ($\lambda_{\text{ex}} = 320 \text{ nm}$) of the Fe^{3+} -EuL samples obtained at different reaction times.

3. PXRD Analysis

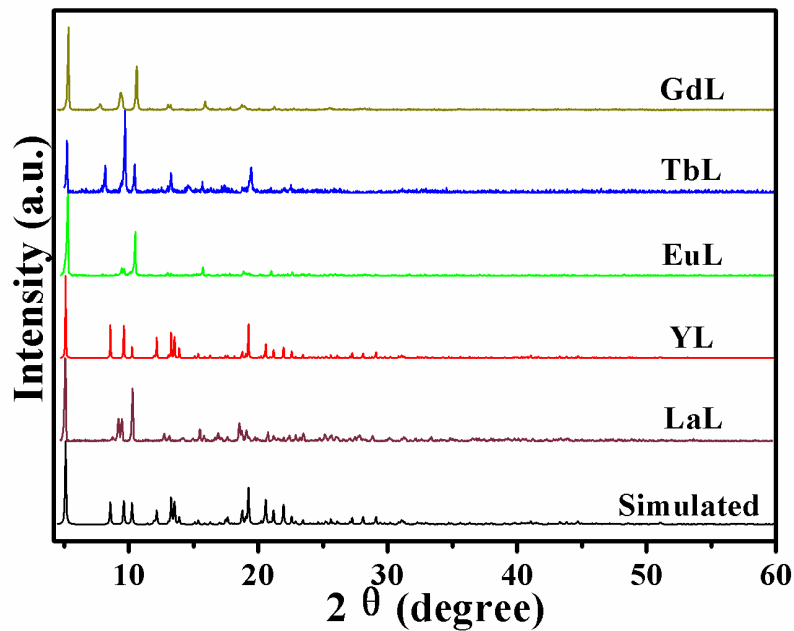


Fig. S3 Powder XRD patterns of compounds LnL ($\text{Ln} = \text{La}, \text{Y}, \text{Eu}, \text{Tb}, \text{Gd}$).

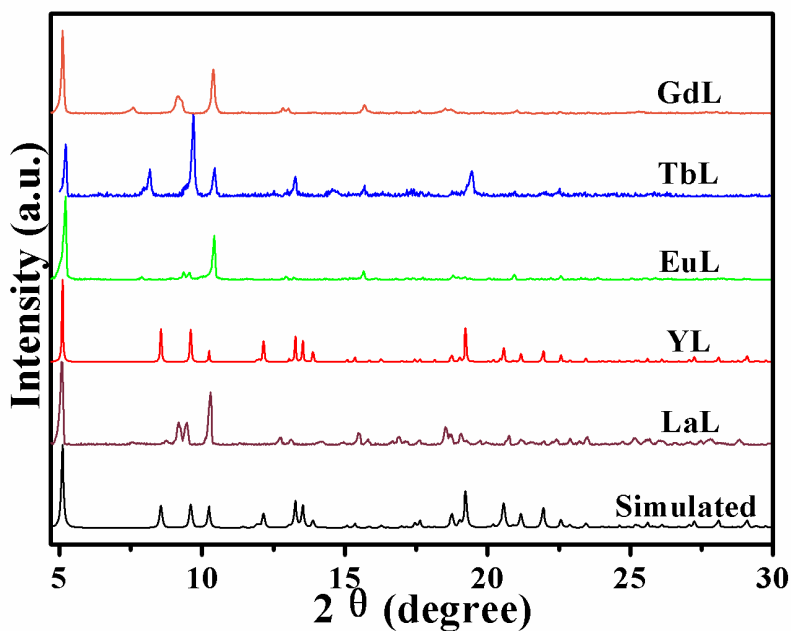


Fig. S4 Powder XRD patterns of compounds **LnL** ($\text{Ln} = \text{La}, \text{Y}, \text{Eu}, \text{Tb}, \text{Gd}$) in the range from 5 to 30 degrees. Some trace amount of unknown impurities still exist in **GdL** and **TbL**.

4. TGA analyses

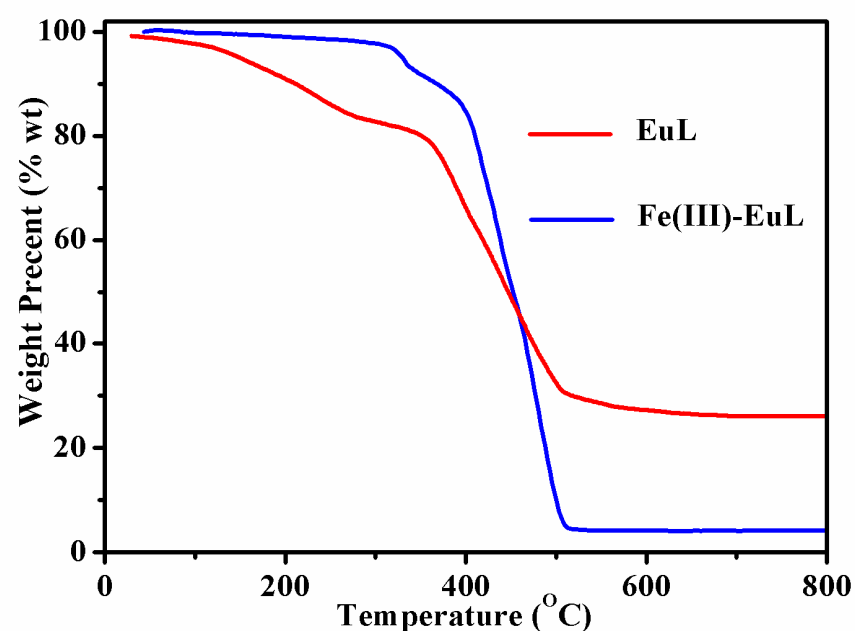


Fig. S5 Thermogravimetric analyses of **EuL** and **Fe(III)-EuL**.